Sea-Level Slopes and Volume Fluxes Produced by Atmospheric Forcing in Estuaries: Chesapeake Bay Case Study

Authors: Salas-Monreal, David, and Valle-Levinson, Arnoldo

Source: Journal of Coastal Research, 24(sp2) : 208-217

Published By: Coastal Education and Research Foundation

URL: https://doi.org/10.2112/06-0632.1

Journal of Coastal Research	24	2B	208–217	West Palm Beach, Florida	March 2008

Sea-Level Slopes and Volume Fluxes Produced by Atmospheric Forcing in Estuaries: Chesapeake Bay Case Study

David Salas-Monreal*† and Arnoldo Valle-Levinson‡

†Old Dominion University,
Center for Coastal Physical Oceanography
768 W 52nd St.
Norfolk, VA 23529, U.S.A.
davsalas@uv.mx

‡University of Florida
Department of Civil and Coastal Engineering
P.O. Box 116580
Gainesville, FL 32611-6580, U.S.A.
arnoldo@coastal.ufl.edu

ABSTRACT

SALAS-MONREAL, D. and VALLE-LEVINSON, A., 2008. Sea-level slopes and volume fluxes produced by atmospheric forcing in estuaries: Chesapeake Bay case study. *Journal of Coastal Research,* 24(2B), 208–217. West Palm Beach (Florida), ISSN 0749-0208.

Time series at eight locations in Chesapeake Bay and the adjacent inner shelf were used to determine the relative influence of the wind and barometric pressure effects on subtidal sea-level variability and slopes in the estuary. Special emphasis was placed on the lower Chesapeake Bay, where inverse barometric effects accounted for up to 32% of the subtidal sea-level variations, and wind forcing accounted for more than 67% of the variance. The wind frequency from any given direction varied from one station to another due to the nonsynoptic characteristics of atmospheric pressure in Chesapeake Bay. In the northern bay, northwesterly winds were most frequent in winter, and southerly winds were most frequent in summer. In the southern bay, northeasterly winds were most frequent in fall and winter, and southwesterly winds dominated in the summer. These winds produced sea-level responses as follows: northeasterly winds caused water to pile up in the southwestern corner of the bay, whereas southwesterly winds produced water-level depressions in the same area. This study is one of the few to document the influence of atmospheric pressure gradients on estuarine sea-level slopes. It was found that atmospheric pressure gradients produced sea-level slopes of the same order of magnitude (10^{-7}) as those induced by westerly–easterly winds. In contrast to previous studies, the volume fluxes calculated here, with geostrophy, geostrophy plus wind stress, and the continuity constraint, showed drainage of the bay with northerly and northwesterly winds and filling of the bay with southeasterly winds.

ADDITIONAL INDEX WORDS: *Subtidal variability, sea level, wind stress, geostrophic velocity, Chesapeake Bay.*

INTRODUCTION

Circulation in estuaries can be affected by atmospheric forcing, which alters barotropic pressure gradient, *i.e.,* the sea-level slope. The typically observed seaward barotropic pressure-gradient force in estuaries can be modified by wind-induced sea-level slopes, barometric pressure, and steric (thermosteric plus halosteric) effects from heating and cooling processes. The aim of this study was to explore the roles of different atmospheric influences on the estuarine barotropic pressure gradient in Chesapeake Bay and, specifically, to advance the understanding of wind and inverse barometric effects on sea-level variability and sea-level slopes, and their relevance on volume fluxes at the Chesapeake Bay mouth. Fulfilling these objectives will be relevant to predictions of sea-level changes and volume fluxes in the Chesapeake Bay and other estuarine systems of similar dimensions.

Wind stress has been identified as the main producer of subtidal sea-level variability in several coastal basins, including the Sado Estuary (MARTINS *et al.,* 2001), Narragansett Bay (WEISBERG and STURGES, 1976), San Francisco Bay (WALTERS and GARTNER, 1985), and the North Inlet, South Carolina, where the subtidal water-level variability is quite sensitive to changes in wind direction (KJERFVE *et al.,* 1978). In the Chesapeake Bay, northeasterly winds cause water level to rise in the southwestern corner of the bay due to water transport from coastal and upper bay areas (VALLE-LEVINSON *et al.,* 2001). Southwesterly winds that dominate during summer (PARASO and VALLE-LEVINSON, 1996) produce the opposite scenario on the sea level and sea-level slopes. In most of the previous studies, the subtidal sea level was correlated to wind but not to other forces. One of the innovative aspects of this study is the isolation of barometric and wind-forcing effects on subtidal sea-level variability and their influence on the estuarine barotropic pressure gradient at different locations throughout Chesapeake Bay.

In basins with large atmospheric pressure variability, the sea-level response to changes in atmospheric pressure cannot be neglected. Several coastal studies have revealed the importance of the inverse barometric effect on subtidal sea-level variability (SHENG *et al.,* 1998; VALLE-LEVINSON *et al.,* 2001), which in some cases can be as important as the tidal signal

DOI:10.2112/06-0632.1 received 08 January 2006; accepted in revision 20 November 2006.

* Present address: Universidad Veracruzana, Centro de Ecologia y Pesquerias, 617 Rio Jamapa, Boca del Rio, VER 94290, Mexico.

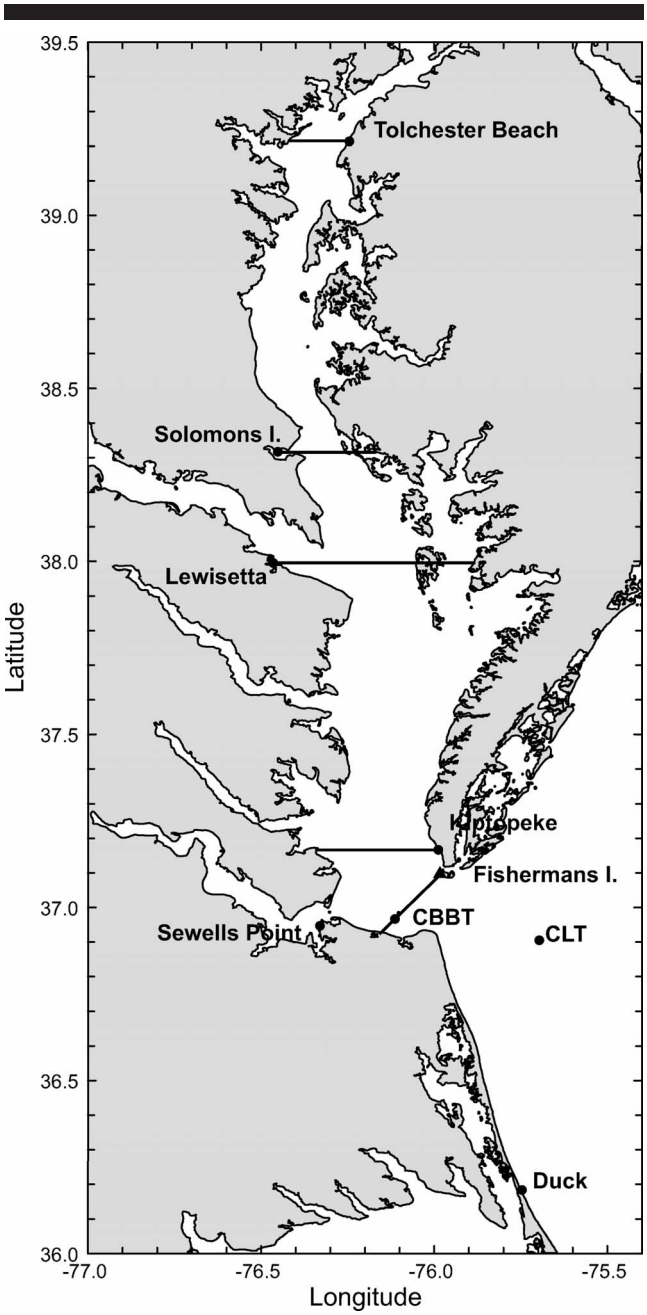

Figure 1. Chesapeake Bay and positions of the eight stations, inside and outside the bay (●). The lines represent the boundaries for each segment used in the calculation of volume fluxes.

(WISEMAN *et al.,* 1988). In some marginal seas, the subtidal sea-level variability is dominated by the inverse barometric effect, as in the Aegean Sea (TSIMPLIS and VLAHAKIS, 1994) and Western Mediterranean (CANDELA, 1991). In the Chesapeake Bay, the inverse barometric effect on sea level has been found to be smaller than the wind stress effects but not negligible (PARASO and VALLE-LEVINSON, 1996). This effect may be as important as the wind-forcing effect in the upper bay (SPITZ and KLINCK, 1998). However, observational studies of estuaries and bays regarding the inverse barometric effect are scarce (KIM *et al.,* 1996). A comprehensive scrutiny of inverse barometric effects throughout Chesapeake Bay is still lacking.

Table 1. *Station locations in Maryland (MD), Virginia (VA), and North Carolina (NC).*

Station Number	Station Name	Latitude (N)	Longitude (N)
8573364	Tolchester Beach, MD	39°12.8′	76°14.7′
8577330	Solomons Island, MD	38°19.0′	76°27.1′
8635750	Lewisetta, VA	37°59.7′	76°27.9′
8632200	Kiptopeke, VA	37°10.0′	75°59.3′
8638610	Sewells Point, VA	36°56.8′	76°19.8′
8638863	Chesapeake Bay Bridge Tunnel (CBBT), VA	36°58.0′	76°6.8′
8638979	Chesapeake Light Tower (CLT), VA	36°54.3′	75°41.8′
8651370	Duck, NC	36°11.0′	75°44.8′

The importance of wind and inverse barometric effects on sea level and sea-level slopes needs to be studied in detail in order to improve understanding of estuarine hydrodynamics. In this study, the barometric pressure effect was calculated at eight sea-level locations throughout Chesapeake Bay (Figure 1). This effect was subtracted from the total subtidal sea level, and the remaining variability was attributed to the wind, because of the high correlation (typical correlation coefficients of 0.8) and coherence at low frequencies between the modified subtidal sea level and the wind. Finally, volume fluxes or the rate of change of volume throughout the bay mouth were calculated with the geostrophic approximation, and with geostrophy modified by wind stress. These calculations were compared with those obtained from volume fluxes derived from the continuity equation, using the time rate of change of sea level. When compared to previous studies on subtidal variability in the Chesapeake Bay (GARVINE, 1985; GOODRICH, 1988; PRITCHARD, 1965; WANG, 1979; WANG and ELLIOT, 1978), this study is distinguished by the assessment of both wind and inverse barometric effects throughout the estuary using a year-long data set. The most important contribution is the evaluation of the relative influence of these effects on subtidal sea-level slopes and net volume fluxes.

DATA AND PROCEDURES

Hourly time series of sea level, atmospheric pressure, wind velocity, salinity, temperature, and density of seawater at eight stations (Figure 1, Table 1), within and outside the Chesapeake Bay, were used to determine the relative influence of wind and barometric pressure effects on sea-level variability and sea-level slopes. Data from the year 2000 were used because of the availability of hourly time series of salinity and temperature data at several stations, which allowed density calculations to be used to estimate the barometric pressure effect on sea levels. These series were mainly obtained from stations maintained by the National Oceanic and Atmospheric Administration (NOAA). The temperature derived from the tide gauge stilling wells may have overestimated ambient temperature under extended periods of direct

Table 2. *Surface areas and Coriolis parameter used for each segment shown in Figure 1.*

Segment	Surface Area (m^2)	Coriolis Parameter (s^{-1})
Head–Tolchester Beach	319×10^6	9.2483×10^{-5}
Tolchester Beach–Solomons Island	1484×10^6	9.1314×10^{-5}
Solomons Island–Lewisetta	893×10^6	9.0100×10^{-5}
Lewisetta–Kiptopeke	2585×10^6	8.8944×10^{-5}
Kiptopeke–Chesapeake Bay Mouth	552×10^6	8.7904×10^{-5}

sunlight. Salinity data from Chesapeake Bay Observing System (CBOS) stations were used to fill gaps at Tolchester Beach and Solomons stations. Monthly conductivity-temperature and depth (CTD) data series obtained by the Center for Coastal Physical Oceanography (CCPO) across the lower bay were also used to fill in salinity and temperature gaps at the Chesapeake Bay Bridge Tunnel (CBBT) and Kiptopeke. CTD data from the Naval Atlantic Meteorology and Oceanography Center (NAMOC) near Duck station (DUCN7) were used to fill in salinity and temperature gaps at Duck station. Wind data from the Chesapeake Light Tower (CLT) were used to calculate wind stress. The zero-height sea level was corrected by subtracting the annual mean from each year-long data set. The corrected data were then used to calculate the sea-level slope between stations.

Gaps greater than 3 h were filled with the best linear regression between nearby stations with existing data, while gaps less than or equal to 3 h were filled with linear interpolations between successive data. The barometric pressure series from Chesapeake Bay Bridge Tunnel was used to fill in the missing series at Kiptopeke station because of its proximity in the lower bay. The salinity time series at Kiptopeke station was constructed with CCPO available monthly data series near Fishermans Island (37°11.118′ N, 76°0.942′ W) and interpolated hourly with a linear regression between Fishermans Island and Chesapeake Bay Bridge Tunnel. The values for the linear regression, slope of 0.8956 and intercept of 4.4566, indicated higher sea-surface salinity at Fishermans Island than at Chesapeake Bay Bridge Tunnel. This was because the Coriolis effect deflects salty water to the north part of the bay mouth, while less saline water exists mainly at the southern part of the bay mouth (Paraso and Valle-Levinson, 1996). Because this study concentrated on subtidal variability, frequencies higher than 0.03846 cycles per hour (period of 26 h) were filtered out from sea level, water temperature, salinity, atmospheric pressure, and wind-velocity records, using a low-pass cosine-Lanczos filter.

In order to estimate and subtract the barometric pressure effect from sea-level variability, it was necessary to analyze a total differential of the pressure. This was done by using the hydrostatic equation, following Gill (1982):

$$\Delta\eta_a = -\frac{1}{\rho g}\Delta P_a, \tag{1}$$

where η_a is the subtidal water level produced by atmospheric pressure (P_a), ρ is the seawater density, and g is the acceleration due to gravity. Once the percentage of variability attributed to the inverse barometric ($\Delta\eta_a$) effect was determined, the remaining variability was assumed to be produced by the wind. This assumption was tested with the coherence between the remaining sea level and the wind. Such an approach allowed quantification of the main factors affecting the subtidal sea-level variability.

Table 3. *The mean depth used for each station and the cross-sectional areas shown in Figure 1, as well as the percentage of tidal variance at each station.*

Stations	Depth (m)	Transverse Area (m^2)	% Tidal Variance
Tolchester Beach	5.30	0.75×10^4	49.64
Solomons Island	15.00	2.04×10^5	41.12
Lewisetta	8.50	3.09×10^5	44.70
Sewells Point	4.47	N/A	70.22
Kiptopeke	7.70	2.29×10^5	77.17
Chesapeake Bay Bridge Tunnel	9.14	2.12×10^5	72.93
Duck	15.00	N/A	82.31
Chesapeake Light Tower	18.30	N/A	N/A

Volume fluxes were calculated once the variation due to the inverse barometric effect was removed from subtidal sea levels. These estimated volume fluxes were produced by wind and/or by sea-level slopes. Slopes, in turn, were calculated using subtidal sea levels and the distance between contiguous stations. In addition, the continuity constraint was used to obtain a more reliable estimate of volume fluxes than those derived from the geostrophic or from the geostrophic approximation modified by wind stress. For this purpose, the bay was divided into five segments according to data availability, each of which had one or more tide gauges (Figure 1, Tables 1 and 2). This partition is valid under the assumption that subtidal water level has the same variation in the entire segment. The rate of change of volume ($\Delta Vol_i/\Delta t$) was estimated following the methods of Vieira (1985) and Monreal-Gomez and Salas-De-Leon (1990):

$$\frac{\Delta \mathrm{Vol}_i}{\Delta t} = A_{S_i}\frac{\lfloor \eta_i(t_{j+1}) - \eta_i(t_j)\rfloor}{\Delta t}, \tag{2}$$

where Vol_i is the volume of the ith segment, A_{Si} is its surface area (Table 2), and $\eta_i(t_j)$ is the subtidal water level of the ith segment at time t_j. Sewells Point and Chesapeake Bay Bridge Tunnel stations were considered in the same segment because of their sea level, water temperature, salinity, and wind-velocity coherence. The subtidal sea level for this segment was taken as the average elevation change recorded by the two tide gauges. The rate of change of volume for each segment was determined with Equation (2), and then the time rate of change of the bay volume was obtained by adding all individual segments.

In addition, sea-level slopes were used to estimate geostrophic volume fluxes (V_g) in $m^3\ s^{-1}$ (Gill, 1982), at the Chesapeake Bay entrance:

$$V_g = A_t u = -\frac{gA_t}{f}\frac{\Delta\eta}{\Delta y}, \tag{3}$$

where A_t is the bay entrance cross-sectional area (Table 3), u

is the geostrophic velocity perpendicular to the entrance,($\Delta\eta/\Delta y$) is the cross-estuary sea-level slope, and f is the Coriolis parameter (Table 2). The volume fluxes (V_{qg}) were also obtained from geostrophy plus cross-estuary wind stress (τ_s^y):

$$V_{qg} = A_t u = -\frac{gA_t}{f}\frac{\Delta\eta}{\Delta y} + \frac{\tau_s^y A_t}{f\rho h} \quad (4)$$

where h is the mean depth of the transect (Table 3). The cross-estuary wind stress was used because it dominates over the along-estuary wind stress component in the geostrophic approximation. All the variables used to calculate sea-level variations, sea-level slopes, and volume fluxes were filtered to illustrate subtidal fluxes for each segment. Equations (3) and (4) are applied under the assumption that the timescale of variations of the subtidal currents and the frictional decay time is $>1/f$, *i.e.*, >3 h, which is a reasonable assumption. The geostrophic velocity and the geostrophy velocity modified by wind stress were compared with those calculated from the continuity equation to analyze the dynamical implications of the different estimates.

Finally, a complex regression of the wind and the current, obtained with the continuity constraint estimate, was carried out to elucidate the transfer factor (A) and the veering angle (θ) between them. This was done following the methods of Prandle and Mattews (1990) and Souza *et al.* (1997):

$$U(t) - U_0 = aW(t), \quad (5)$$

where U is the total nontidal velocity at time t. In turn, U_0 is the non-wind-forced residual, W is the wind velocity, and a is the complex coefficient. The complex coefficient, $a = |a|e^{+i\theta}$, can be expressed in terms of the transfer factor as $A = |a|$.

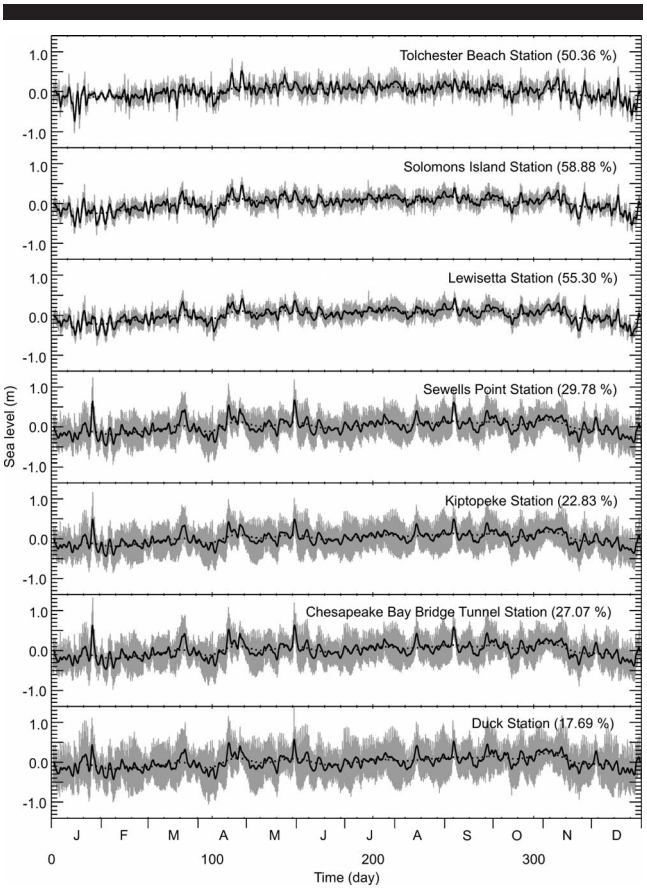

Figure 2. Total (gray) and subtidal sea level throughout the year 2000. Subtidal sea levels were obtained using a low-pass filter for 26 h (solid line) and 20 d (dashed line). The percentages refer to 26 h subtidal sea-level variance.

RESULTS AND DISCUSSION

Subtidal sea levels at Tolchester Beach, Solomons Island, and Lewisetta stations in the upper bay where highly correlated. Sewells Point, Kiptopeke, and Chesapeake Bay Bridge Tunnel, in the lower Chesapeake Bay, and Duck Station, outside the bay, were highly correlated among each other but differed from the upper bay stations. Still, the percentage of subtidal sea-level variability related to total variability differed between contiguous stations (Figure 2). In the upper Chesapeake Bay, subtidal sea-level variations explained more than 50% of the total oscillations. In this region, subtidal variance was larger than tidal variance (Table 3). In contrast, in the lower bay, tidal fluctuations dominated close to the mouth, and only 20% to 30% of the variance was produced by subtidal effects. This fact was attributed to the proximity of the lower bay stations to tidal forcing and the proximity of the upper bay stations to a virtual amphidromic point located between Tolchester Beach and Solomons Island Stations (Browne and Fisher, 1998). The greatest tidal influence on sea level within the bay (77%) was found at Kiptopeke in the northern Chesapeake Bay mouth. This was the sampling site most sheltered from energetic northeasterly and northwesterly winds.

A small fraction (<1%) of the subtidal variability was attributed to steric effects, produced by thermal expansion and haline contraction. The weak subtidal variability attributed to steric effects enhanced the significance of the wind stress and the inverse barometric effect in the subtidal variability. It is noteworthy that steric influence was non-negligible over seasonal scales; it produced sea-level amplitude variations close to 10 cm (Figure 2). The highest subtidal sea levels were observed in the summer, and the lowest were observed in winter in response to thermal expansion effects. In addition, there were intraseasonal variations (dashed line in Figure 2) related to major freshwater pulses into the bay. Continuous freshwater supplies raised the subtidal water level in the upper bay, and reduced the density variance. In the lower bay, the coastal water exchange at the mouth should have accounted for the highest thermohaline variation. However, the along-bay sea-level slope associated with steric effects was negligible.

A much more significant portion of subtidal variability in sea level, relative to steric effects, was produced by the inverse barometric effect (Figure 3). In most stations, this effect explained about 22% of the subtidal variance. Results show that its relative effect, compared to total subtidal variability, was smaller in the upper bay than in the middle and lower

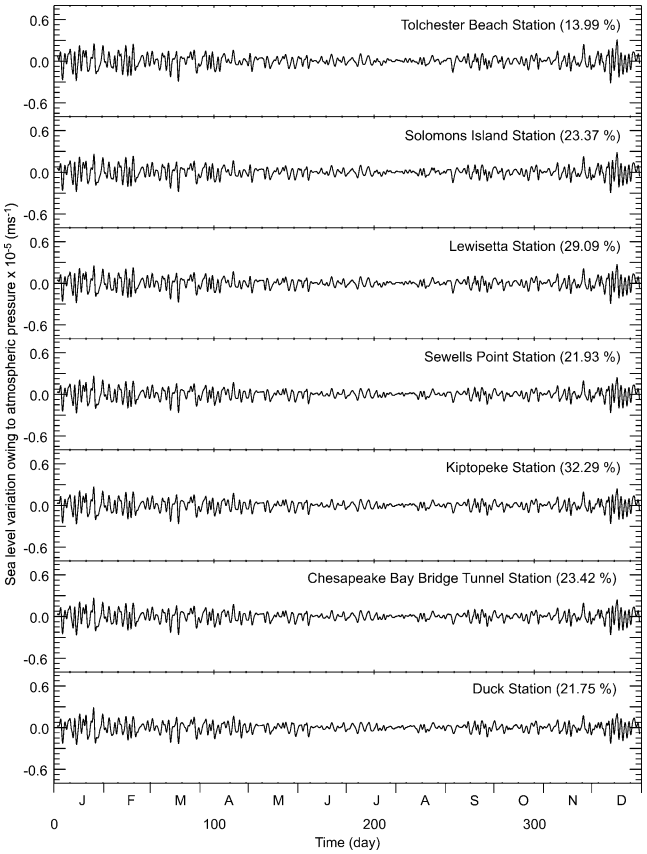

Figure 3. Subtidal sea-level variation owing to atmospheric pressure throughout the year 2000. The percentages refer to subtidal sea-level variation variance.

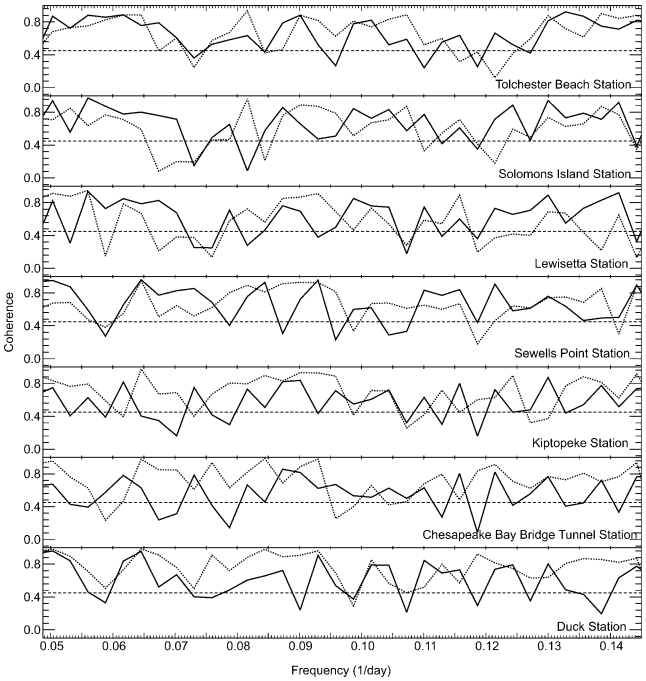

Figure 4. Coherence between wind-velocity components and subtidal sea level using the north-south component (solid line) and the east-west component (dotted line) at 80% confidence level (dashed line).

bay. These results are different from those found by SPITZ and KLINCK (1998). At Tolchester Beach station, in the upper bay, the inverse barometric effect accounted for less than 14% of the subtidal variability, whereas at Kiptopeke station, in the lower bay, it accounted for 32% of the subtidal variability (Figure 3). Thus, the relative effect of the inverse barometric effect increases from the upper to the lower bay and tends to be more variant in winter (Figure 3). The relative influence of the inverse barometric effect on total subtidal sea-level variability was most evident in winter, during specific events like storms and frontal passages. During these events, extreme lows in atmospheric pressure caused large subtidal changes in sea level. The sea-level slope generated by the atmospheric pressure gradient was frequently caused by higher atmospheric pressure in the upper bay than in the lower bay. Those atmospheric pressure gradients usually generated a negative sea-level slope on the order of 10^{-7}. The sea-level variability attributed to atmospheric pressure was highly correlated among stations with a small phase lag of ~11 h, which was attributed to spatially variable atmospheric pressure gradients along the bay. For instance, sea-level perturbations produced in the upper bay, traveling as long waves over ~6.5 m depth, will be felt in the lower bay, 320 km away, in approximately 11 h. One of the most relevant findings of this analysis was that the inverse barometric effect in Chesapeake Bay, and perhaps in any large estuary (>120 km), should be included in subtidal sea-level analysis, and not only in analysis of subtidal sea-level variability, but also in determination of subtidal sea-level slopes.

Besides the barometric effects, subtidal sea-level variations were also caused by wind forcing. In fact, the remaining subtidal sea-level variation in the bay was attributed to wind stress because of their high coherence (Figure 4). At lower bay stations, the coherence between subtidal sea level and the east-west wind component was higher than the coherence between subtidal sea level and the north-south wind component, at frequencies higher than 0.125 cycles per day (cpd) (periods smaller than 8 d). This was attributed to the orientation of the bay mouth, which, for instance, allowed a faster sea-level depression with westerly than with southerly winds. In the upper bay, the coherence was higher between the north-south wind component and the subtidal sea level at frequencies less than 0.07 cpd. In most stations, the wind-induced subtidal variability explained more than 67% of the variance (Figure 5), up to 86% at Tolchester Beach station and about 77% elsewhere. The largest subtidal sea-level variance attributed to wind stress was found in the upper bay, owing to more sustained winds than in the lower bay, although stronger winds were measured in the lower bay than in the upper bay.

The percentage of the sea-level variance attributed to the wind, and the atmospheric pressure gradient was corroborated by an empirical orthogonal function (EOF) analysis (*e.g.*,

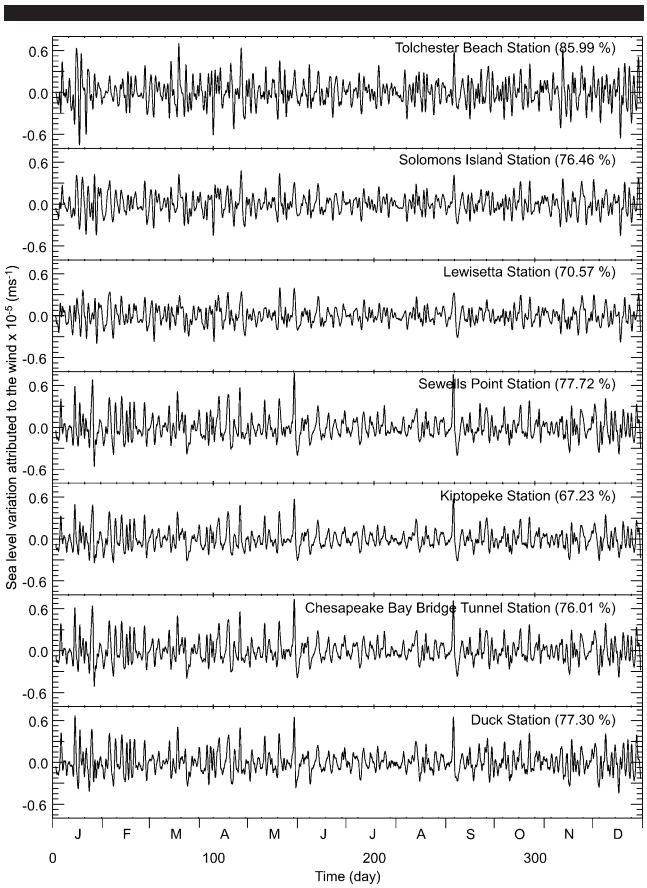

Figure 5. Subtidal sea-level variation attributed to wind effects throughout the year 2000. The percentages refer to subtidal sea-level variation variance.

Table 4. *Percent of total variance explained by each of the modes obtained via an emprical orthogonal function (EOF) analysis on the subtidal sea level.*

Stations	Mode 1	Mode 2	Mode 3
Tolchester Beach	84.0	15.6	0.4
Solomons Island	72.0	27.6	0.4
Lewisetta	67.8	31.9	0.3
Sewells Point	73.5	25.2	1.3
Kiptopeke	63.2	35.4	1.4
Chesapeake Bay Bridge Tunnel	72.9	25.6	1.5

ELLIOTT, 1978; WALLACE and DICKINSON, 1972). The EOF analysis is a decomposition of the data set in terms of orthogonal functions that are determined from the data. This analysis was performed for the subtidal series. The values obtained for each station (Table 4) showed the dominance of the first mode, explaining between 84% and 63% of total variance. The first mode was correlated with the wind speed ($R = 0.8$). In turn, the second mode was correlated with the inverse barometric effect and explained up to 35% of total variance. The third mode did not contribute significantly to the variance and can be considered as noise for the purpose of this study. The two methods used in this study to calculate the percentage of the variance attributed to wind, inverse barometric effect, and steric effects suggested the dominance of the wind (84%–63%) in the total sea-level variance. However, the inverse barometric effect could not be neglected, since it contributed effectively to total sea-level variance (15%–35%).

Thirty-five extreme sea-level variation events identified throughout the year 2000 were mainly attributable to wind forcing (Figure 6). Out of those extreme events, 60% were associated with net volume inflows. Net volume outflows (Figure 6a), calculated with the continuity equation, were correlated with northwesterly ($R = 0.68$, where R is the correlation coefficient) or southwesterly ($R = 0.62$) winds. Net volume inflows were correlated with northeasterly ($R = 0.57$) or southeasterly ($R = 0.76$) winds, since northeasterly and southwesterly winds are the main producers of bay/coastal water exchange. Extreme net volume fluxes were associated with extreme sea-level slope events during specific winds conditions, which showed spatial variability in the bay.

Water-level slopes between the upper and the lower bay were up to 6×10^{-6} (Figure 6b) and were similar to those across the Chesapeake Bay mouth (Figure 6c) during strong (>10 m/s) and synoptically coherent wind conditions (Figure

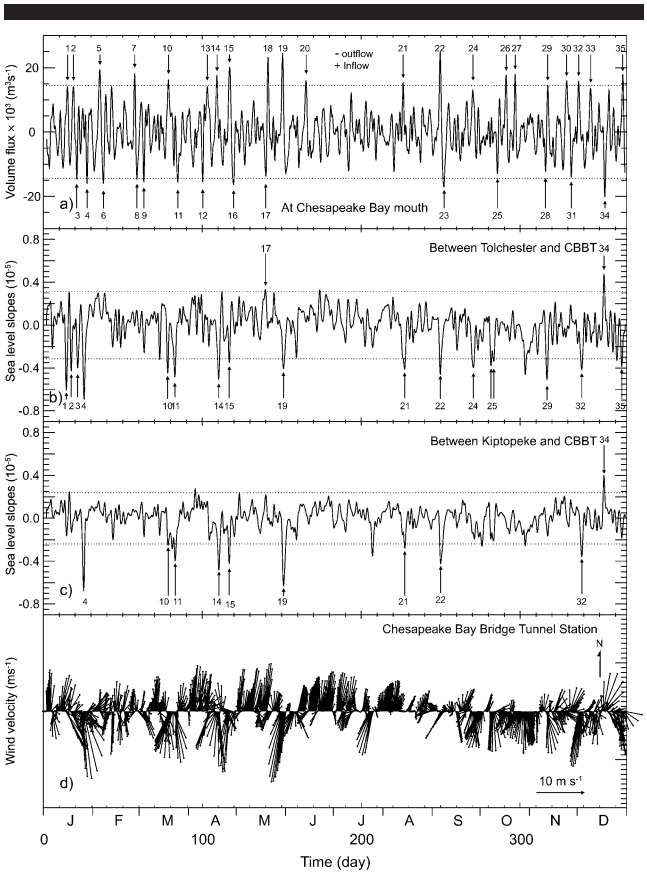

Figure 6. (a) Extreme volume fluxes, (b) slopes between Tolchester and CBBT, (c) slopes between Kiptopeke and CBBT, and (d) wind velocity at CBBT throughout the year 2000.

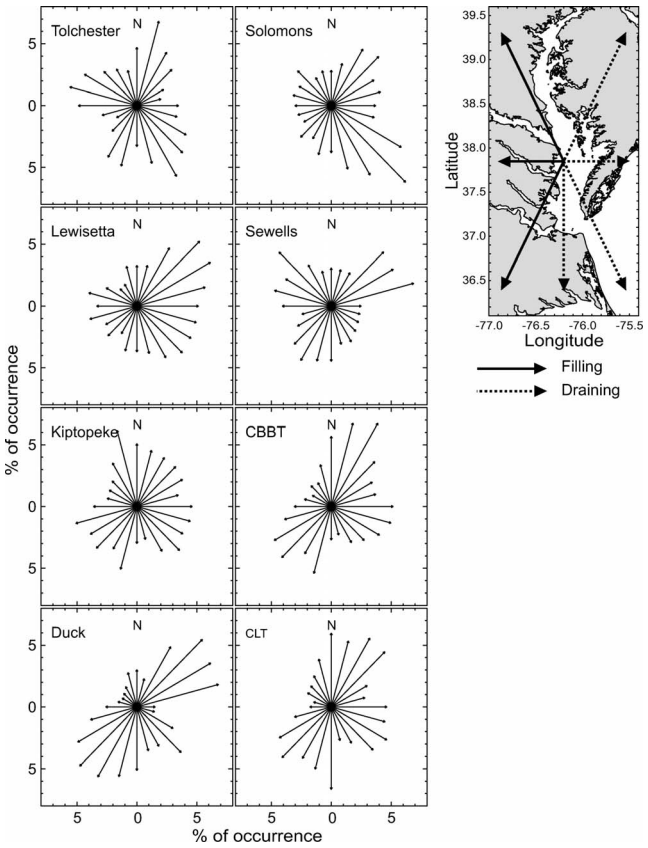

Figure 7. Percentage of wind direction occurrence, every 15°, throughout the year 2000, and the wind-induced draining and filling.

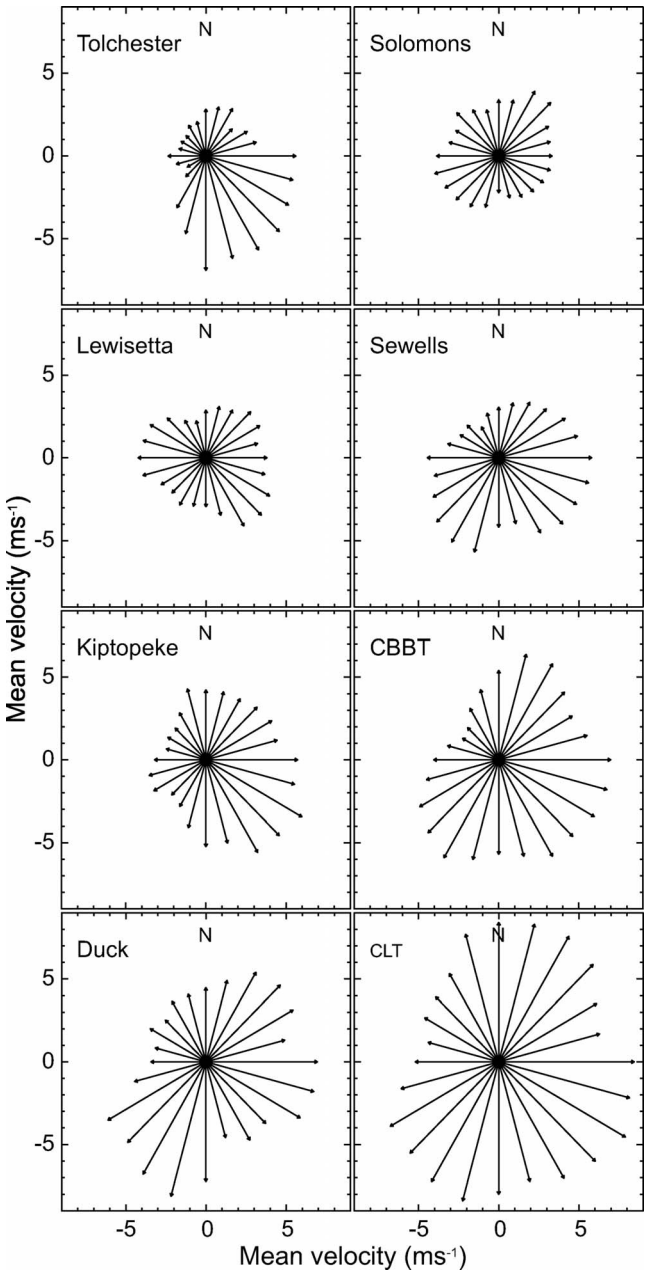

Figure 8. Mean wind velocity, every 15°, throughout the year 2000.

6d). For spatially variable winds, sea-level slopes across the bay were larger than along-bay slopes. Above 84% of extreme wind-induced sea-level slopes were negative (Figure 6), *i.e.,* upward slopes toward the south caused by a frequently higher atmospheric pressure in the upper bay than in the lower bay that drove winds southward.

Variations in wind direction (Figure 7) and speed (Figure 8) among meteorological stations throughout the bay exhibited a nonsynoptic character attributed to the length of the bay (~320 km). The lower bay had predominant northeasterly and southwesterly wind directions, and the northeasterly wind was the strongest. The upper bay had predominant northwesterly and southwesterly wind directions, and the strongest was the northwesterly wind. The wind speed decreased considerably from the southern to the northern bay owing to land friction over a narrower bay. The strongest winds were observed at Chesapeake Light Tower, and the weakest winds were observed at Tolchester Beach station (Figure 8). A combination of northerly wind in the upper bay with a strong northwesterly wind (>8 m s^{-1}) in the lower bay produced the fastest drainage of Chesapeake Bay (Figure 7).

Sea-level slopes associated with southeasterly wind pulses were up to 3×10^{-6}, with sea level decreasing from head to mouth of the bay (Figures 9a and 9b). The largest slopes of up to -6×10^{-6} along the bay and -7×10^{-6} across the mouth were associated with northeasterly winds (Figure 9c), which were the most common and energetic winds in the lower bay. Northwesterly winds (Figure 9d) produced sea-level depression in the upper bay and sea-level set-up in the lower bay as previously documented by VALLE-LEVINSON *et al.* (2001). Easterly winds produced sea-level set-up and westerly winds caused sea-level set-down in the lower bay, owing to bay/coastal interaction. However, the upper bay was not significantly affected by those winds because the water could not be flushed out or filled in as in the lower bay. During westerly or easterly wind conditions (Figure 9e), the slopes

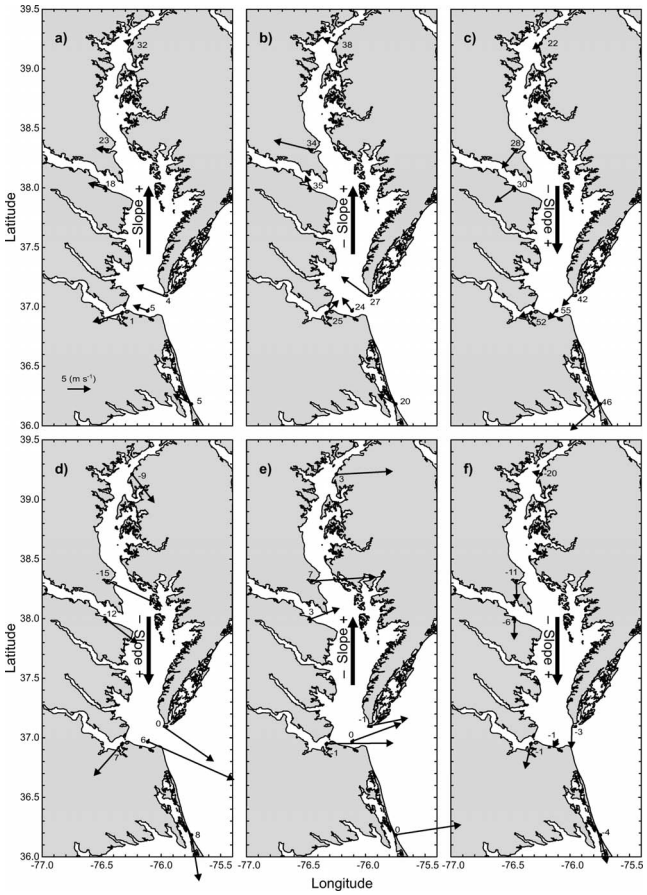

Figure 9. Six extreme volume flux events through the Chesapeake Bay mouth showing the average during a two day period of sea level (cm) (numbers) and wind (light arrows) and slope (dark arrows). The events are: (a) the 25th (October 17, 2000), (b) the 12th (April 26, 2000), (c) the 18th (September 6, 2000), (d) the 1st (January 21, 2000), (e) the 7th (March 3, 2000), and (f) the 13th (April 28, 2000).

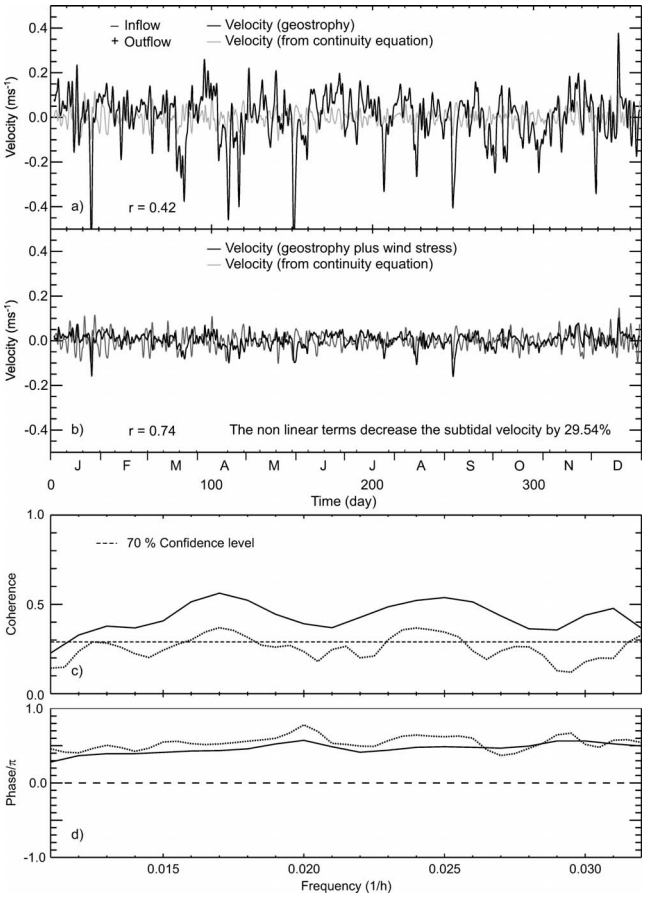

Figure 10. The mean velocity at Chesapeake Bay mouth, calculated using the momentum equation and (a) geostrophy or (b) the geostrophic approximation modified by the wind stress. (c) The coherence between velocities calculated with continuity and geostrophy (dotted line) and between continuity and geostrophy plus wind stress (solid line), and (d) the phase between velocities calculated with continuity and geostrophy (dotted line) and between continuity and geostrophy plus wind stress (solid line).

produced by the wind were of the same order of magnitude (10^{-7}) as those produced exclusively by the atmospheric pressure gradient from the head to the mouth of the bay.

Flow driven by northerly winds (Figure 9f) caused water to set-up in the lower bay and produced sea-level depression in the northernmost part of the bay, creating slopes of up to -6×10^{-6}. Water set-up at the southernmost part of the bay during northerly winds, as shown by the slopes, was the combination of southward flow inside the bay and coastal inflow. Southerly wind conditions created the opposite sea-level slope scenario: sea-level depressions in the southern part of the bay and water set-up in the northernmost part of the bay. During extreme sea-level slope events, winds were highly energetic (Figure 6), producing slopes on the order of 10^{-6}, which is one order of magnitude higher than those induced by barometric effects. During westerly or easterly wind conditions, the slopes produced by the wind were of the same order of magnitude (10^{-7}) as those produced exclusively by the atmospheric pressure gradient from the head to the mouth of the bay. These wind-induced slopes were smaller than those produced by northerly or southerly winds because of the reduced fetch across the bay. The development of large cross-sectional slopes may also be hampered during westerly winds by the mouth opening, where there is no coast where water can pile up.

Observed extreme sea-level slopes were used to estimate geostrophic and geostrophic plus wind stress volume fluxes at the Chesapeake Bay mouth. These values were compared to those obtained with the continuity constraint (Wong, 1994). One of the advantages of the continuity constraint method when compared to others (*e.g.,* Salas-Monreal, 2002; Simpson *et al.,* 2001) is the possibility of calculating the volume fluxes with only one data series, *i.e.,* sea level. According to the continuity-constrained calculations, southwesterly winds produced net volume outflows, whereas northeasterly winds produced net volume inflows and water set-up at the southwestern corner of the bay. The slope produced across the mouth by northeasterly winds (-7×10^{-6})

suggested a cross-sectional mean geostrophic velocity at the Chesapeake Bay mouth of up to 0.6 m s^{-1}, which resulted in the strongest geostrophic flows (Figure 10a). For both southwesterly and northeasterly wind directions, a compensatory flow developed after the winds relaxed, in response to the barotropic pressure gradient established by the wind. Although northeasterly and southwesterly winds induced the largest sea-level slopes, the biggest sea-level changes and highest volume outflows were found during northwesterly winds, according to the continuity estimates. Southeasterly winds also caused great changes in sea level, mainly in the upper bay, producing net volume inflows of up to 16×10^3 m^3 s^{-1} derived from continuity estimates. Once these winds relaxed, there was a net volume outflow produced by bay/coastal sea-level slopes established by the wind.

Flow driven by northerly winds set-up water in the lower bay (Figure 9f), producing a net outflow instead of inflow, as would be predicted by Ekman transport. It is noteworthy that the volume fluxes produced by northwesterly and southeasterly winds were of opposite sign to those described on the basis of Ekman dynamics. Northwesterly winds actually caused volume outflows, and southeasterly winds drove volume inflows. Easterly winds produced sea-level set-up, and westerly winds caused sea-level set-down in the lower bay, owing to bay/coastal interaction. The three approaches used to estimate volume fluxes: geostrophic, geostrophy plus wind stress, and the continuity constraint predicted inflows with northeasterly, easterly, and southeasterly wind conditions and outflows with northwesterly, northerly, westerly, and southwesterly wind conditions. However, there was a marked difference in net volume fluxes among the three approaches. Geostrophic volume fluxes yielded a low correlation (R = 0.42) with the continuity constraint (Figure 10a). The addition of wind stresses to the equation of momentum (Equation 4) increased the correlation with the continuity constraint (Figure 10b) (R = 0.74), reducing the overestimation considerably.

In order to explore the discrepancy between the volume fluxes produced by northwesterly and southeasterly winds with those expected on the basis of Ekman dynamics, the transfer factor (A) and the veering angle (θ) were calculated (Equation 5) for the Chesapeake Bay mouth stations. This calculation was carried out between the wind and surface currents. Chesapeake Bay Bridge Tunnel (CBBT) station showed a transfer factor of 2.4% with a veering angle of $-12°$. In turn, Kiptopeke, in the northernmost part of the bay mouth, showed a transfer factor of 2% with an associated veering angle of $-17°$. At Sewells Point station, inside the bay, the transfer factor and veering angle were 2.5% and $-8°$, respectively. According to the veering angle, the estuarine buoyant water should be flushed by northwesterly winds and retained by southeasterly winds.

The discrepancy between the volume fluxes obtained with the dynamic estimates (Equations 3 and 4) and the fluxes calculated with the continuity constraint (Equation 2) (Figures 10c and 10d) accounts for ~25%–30% of the variance and was attributed to nonlinearities from bottom stress and advection, which were also found to be relevant in short-term observations in the lower bay (VALLE-LEVINSON *et al.,* 2002). The discrepancy was also attributed to temporal changes in subtidal flows as $<1/f$, where f is the Coriolis parameter. The absence of advection and bottom friction in the momentum equation approximation produced the geostrophic or the geostrophic modified by wind stress velocities to lead the continuity approximation velocities, which reveals the significance of bottom friction in Chesapeake Bay dynamics owing to its shallowness. If friction is added to the momentum approximations, the estimated velocities will respond faster to a change in wind direction.

CONCLUSIONS

Time series of sea level, atmospheric pressure, wind velocity, and water density data throughout the year 2000 obtained from inside and outside Chesapeake Bay were used to determine: (i) the relative influence of wind and barometric pressure effects on sea-level variability and sea-level slopes, and (ii) volume fluxes through the bay mouth with and without the influence of wind stress. The pursuit of these objectives has yielded five conclusions that advance our understanding of atmospheric forcing effects in the Chesapeake Bay, relative to other studies on this topic, and that may be applicable to other large estuaries. (1) Although the magnitude of sea-level variations due to the inverse barometric effects is largest in the upper bay, the percentage of the subtidal variance explained by this effect was highest in the lower bay. In the lower bay, the inverse barometric effect accounted for up to 32% of the variance owing to a relatively greater atmospheric pressure variation when compared to the upper bay. (2) The lower bay had predominant southwesterly and northeasterly wind directions, whereas the upper bay had predominant southwesterly and northwesterly wind directions. The latter was associated with the most energetic winds in every station. (3) The largest sea-level slopes, up to -6×10^{-6} along the bay and up to -7×10^{-6} across the lower bay, were produced by northeasterly and southwesterly winds. During easterly or westerly winds, the slope due to wind was close to the slope caused by atmospheric pressure gradients. (4) The largest extreme sea-level events and volume fluxes were associated with northwesterly winds, producing outflow ten times the mean river discharge. The largest sea-level slopes were followed by high volume fluxes, but the greatest volume fluxes were not necessarily subsequent to large sea-level slopes. (5) Volume fluxes calculated using geostrophy were overestimated relative to those obtained by continuity. The addition of wind stress to the momentum equation increased the match with the continuity constraint (R = 0.74). The volume fluxes obtained with the dynamic approach explained 70% of the fluxes determined with the time rate of change of sea level. The remaining 30% was attributed to short-term variability ($<1/f$) and to nonlinear effects associated with bottom friction and advection.

ACKNOWLEDGMENTS

The National Oceanic and Atmospheric Administration, the Chesapeake Bay Observing System, and the Naval Atlantic Meteorology and Oceanic Center are gratefully acknowledged for providing data. Kate Bosley and Chester E.

Grosch helped in data processing and provided valuable comments. Jorge Castro substantially improved the figures of this paper. Two anonymous reviewers helped to improve the content of this manuscript. This study was funded by the U.S. National Science Foundation grants OCE-9812206 and OCE-9983685, and the Consejo Nacional de Ciencia y Tecnologia, Mexico (CONACyT), through scholarship 149091/178308.

LITERATURE CITED

BROWNE, D.R. and FISHER, C.W., 1998. Tide and tidal currents in the Chesapeake Bay. NOAA Technical Report NOS OMA 3, 84p.

CANDELA, J., 1991. The Gibraltar Strait and its role in the dynamics of the Mediterranean Sea. *Dynamics of Atmospheres and Oceans,* 15(3–5), 267–299.

ELLIOTT, A.J., 1978. Observations of the meteorologically induced circulation in the Potomac Estuary. *Estuarine and Coastal Marine Science,* 6, 285–299.

GARVINE, R.W., 1985. A simple model of estuarine subtidal fluctuations forced by local and remote wind stress. *Journal of Geophysical Research,* 90, 11945–11948.

GILL, A.E., 1982. *Atmospheric-Ocean Dynamics.* New York: Academic Press, 662p.

GOODRICH, D.M., 1988. On meteorologically induced flushing in three U.S. East Coast estuaries. *Estuarine Coastal and Shelf Science,* 26, 111–121.

KIM, B.C.; CHOI, C.B.K., and BYUN, B.K., 1996. The wind speed dependence of oceanic ambient noise level in the shallow water of Sokcho coast. *Ocean Research,* 18(2), 93–99.

KJERFVE, B.; GREER, J.E., and CROUT, R.L., 1978. Low-frequency response of estuarine sea level to non-local forcing. *In*: WILEY, M.L., (ed.), *Estuarine Interactions.* New York: Academic Press, pp. 497–513.

MARTINS, F.; LEITAO, P., and NEVES, R., 2001. 3D modeling in the Sado Estuary using a new generic vertical discretization approach. *Oceanologica Acta,* 24(1), 51–62.

MONREAL-GOMEZ, M.A. and SALAS-DE-LEON, D.A., 1990. Modelo unidimensional de corrientes en Bahia San Quintin, B.C., Mexico. *Geofisica Internacional,* 29(4), 249–257.

PARASO, M.C. and VALLE-LEVINSON, A., 1996. Meteorological influences on sea level and water temperature in the lower Chesapeake Bay: 1992. *Estuaries,* 19(3), 548–561.

PRANDLE, D. and MATTHEWS, J., 1990. The dynamics of nearshore surface currents generated by tides, winds and horizontal density gradients. *Continental Shelf Research,* 10, 665–681.

PRITCHARD, D.W., 1965. *Kinsman's Notes on Lectures on Estuarine Oceanography.* Baltimore, Maryland: Chesapeake Bay Institute and Department of Oceanography, The Johns Hopkins University, 154p.

SALAS-MONREAL, D., 2002. Sea Level Slopes and Volume Fluxes Produced by Atmospheric Forcing in Chesapeake Bay. Norfolk, Virginia: Old Dominion University, M.S. thesis, 81p.

SHENG, J.; WRIGHT, D.G.; GREATBACH, R.J., and DIETRICH, D.E., 1998. CANDIE: a new version of the DieCAST Ocean Circulation Model. *Journal of Atmospheric and Ocean Technology,* 15(6), 1414–1432.

SIMPSON, J.H.; VENNELL, R., and SOUZA, A.J., 2001. The salt fluxes in a tidally-energetic estuary. *Estuarine, Coastal and Shelf Science,* 52, 131–142.

SOUZA, A.J.; SIMPSON, J.H., and SCHIRMER, F., 1997. Current structure in the Rhine region of freshwater influence. *Journal of Marine Research,* 55, 277–292.

SPITZ, Y.H. and KLINCK, J.M., 1998. Estimate of bottom and surface stress during a spring-neap tide cycle by dynamical assimilation of tide gauge observations in the Chesapeake Bay. *Journal of Geophysical Research,* 103(C6), 12761–12782.

TSIMPLIS, M.N. and VLAHAKIS, G.N., 1994. Meteorological forcing and sea level variability in the Aegean Sea. *Journal of Geophysical Research,* 99(5), 9879–9890.

VALLE-LEVINSON, A.; WONG, K.C., and BOSLEY, K.T., 2001. Observations of the wind-induced exchange at the entrance to Chesapeake Bay. *Journal of Marine Research,* 59(3), 391–416.

VALLE-LEVINSON, A.; WONG, K.C., and BOSLEY, K.T., 2002. Effects of Hurricane Floyd on the exchange at the Chesapeake Bay entrance. *Continental Shelf Research,* 22, 1715–1730.

VIEIRA, M.E.C., 1985. Estimates of subtidal volume flux in mid-Chesapeake Bay. *Estuarine, Coastal and Shelf Science,* 21(3), 411–427.

WALLACE, J.M. and DICKINSON, R.E., 1972. Empirical orthogonal representation of time series in the frequency domain. Part I. Theoretical considerations. *Journal of Applied Meteorology,* II, 887–892.

WALTERS, R.A. and GARTNER, J.W., 1985. Subtidal sea level and current variations in the northern reach of San Francisco Bay. *Estuarine, Coastal and Shelf Science,* 21(1), 17–32.

WANG, D.-P., 1979. Subtidal sea level variations in the Chesapeake Bay and relations to atmospheric forcing. *Journal of Physical Oceanography,* 9, 413–421.

WANG, D.-P. and ELLIOTT, A.J., 1978. Non-tidal variability in the Chesapeake Bay and Potomac River: evidence for non-local forcing. *Journal of Physical Oceanography,* 8, 225–232.

WEISBERG, R.H. and STURGES, W., 1976. Velocity observations in the west passage of Narragansett Bay: a partially mixed estuary. *Journal of Physical Oceanography,* 6(3), 345–354.

WISEMAN, W.J., JR.; SCHROEDER, W.W., and DINNEL, S.P., 1988. Shelf-estuarine water exchanges between the Gulf of Mexico and Mobile Bay, Alabama. *American Fisheries Society Symposium,* 3, 1–8.

WONG, K.-C., 1994. On the nature of transverse variability in a coastal plain estuary. *Journal of Geophysical Research,* 99(C7), 14209–14222.

□ RESUMEN □

Series de tiempo de vientos, presión atmosférica, nivel del mar, temperatura, salinidad y densidad del agua fueron usadas para determinar el efecto del viento y del barómetro invertido en la variación submareal a lo largo de la Bahía de Chesapeake (USA). La variación submareal producida por el viento y el efecto del barómetro invertido varía entre estaciones debido a las dimensiones del estuario (~320 km) y a las características no-sinópticas de la presión atmosférica, lo cual produce que la dirección del viento varíe entre estaciones contiguas. En la zona norte de la bahía predominaron vientos del noroeste durante el invierno, mientras que en la zona sur los vientos del noreste fueron dominantes. Sin embargo durante el verano predominaron los vientos del sur en la zona norte y del suroeste en la zona sur. Con vientos dominantes del noreste, el nivel del mar en la zona suroeste de la bahía se incrementó, mientras que con vientos del suroeste se redujo el nivel del mar en la misma región. En la zona sur de la bahía, el efecto del barómetro invertido fue responsable del 32% de la variación submareal, mientras que el viento lo fue en más del 67% de la variación. Este trabajo es uno de los pocos que documentan los efectos del barómetro invertido sobre las pendientes del nivel del mar. Se demostró que con vientos predominantes del este o del oeste, la pendiente producida en el nivel del mar fue del mismo orden de magnitud que la producida exclusivamente por el efecto del barómetro invertido (10^{-7}). Las pendientes del nivel del mar a lo largo de la boca de la bahía fueron usadas para calcular flujos de volumen geostroficos modificados por el esfuerzo del viento, dichos flujos fueron similares a los calculados mediante la ecuación de continuidad ($r = 0.74$). A diferencia de otros trabajos, se demostró que la bahía presentaba flujos de salida con vientos predominantes del norte y noroeste y flujos de entrada con vientos predominantes del sureste.